Conjugating drug candidates to polymeric chains does not necessarily enhance anti-influenza activity

Alyssa M. Larson, [1] Hongmei Wang, [2] Yang Cao, [3] Taijiao Jiang, [4] Jianzhu Chen, [5] and Alexander M. Klibanov [1, 6]

[1]Department of Chemistry, Massachusetts Institute of Technology, Cambridge, MA 02139, U.S.A.

[2]Department of Applied Chemistry, China Agricultural University, Beijing, 100193, P.R. China

[3]College of Life Science, Sichuan University, Chengdu 610064, P.R. China

[4]Institute of Biophysics, National Laboratory of Biomacromolecules, Chinese Academy of Sciences, Beijing 100101, P.R. China

[5]Department of Biology and David H. Koch Institute for Integrative Cancer Research, Massachusetts Institute of Technology, Cambridge, MA 02139, U.S.A.

[6]Department of Biological Engineering, Massachusetts Institute of Technology, Cambridge, MA 02139, U.S.A.

Abstract

Using the plaque reduction assay, relatively simple bicyclic quinone molecules, as well as multiple copies thereof covalently attached to a long polyglutamate-based polymeric chain, were examined as new inhibitors of various naturally occurring strains of influenza A virus. The polymer-conjugated inhibitors were found to have a far greater potency (for some as high as two orders of magnitude when a long spacer arm was employed) than their corresponding parent molecules against the human Wuhan influenza strain. However, such polymeric inhibitors failed to exhibit higher potency compared to their small-molecule predecessors against the human Puerto Rico and avian turkey influenza strains. These observations, further explored by means of molecular modeling, reveal the previously unrecognized unpredictability of the benefits of multivalency, possibly because of poor accessibility of the viral targets to polymeric agents.

Keywords: Polymeric drugs; structure-activity relationship; drug design; conjugation; anti-infectives; polymeric drug carrier; influenza; inhibitor

Introduction

      Influenza A virus is highly transmissible and kills over 250,000 people worldwide each year. In the United States alone, some 20% of the population contracts the virus annually leading to countless missed days of work and school and tens of billions of dollars in associated costs.[1, 2] The two FDA-approved drugs for the treatment of influenza infections, Oseltamivir (Tamiflu™) and Zanamivir (Relenza™), have fallen short of expectations due to their mediocre activity in reducing the symptoms and duration of the infection, as well as emerging resistance in clinical isolates.[3, 4, 5] Thus new, more effective anti-influenza therapeutic agents are greatly needed.

      One proposed strategy for generating more potent inhibitors of influenza is to utilize the benefits of *multivalency*.[2, 4, 6-11] Conjugating multiple copies of influenza inhibitors to a flexible polymeric chain has been shown to result in multivalent interactions between the polymer-attached inhibitors and the viral surface receptor proteins.[2, 4, 6-11] These enhanced interactions, in turn, lead to a much stronger binding compared to that of the small-molecule parents stemming from favorable entropic factors; additionally, water-swollen polymeric chains may sterically hinder physical contacts between the virus and the target cell.[6]

      The foregoing benefits of multivalency for binding to influenza virus have been demonstrated for viral surface proteins with the natural ligand of hemagglutinin, *N*-acetylneuraminic (sialic) acid, and with the neuraminidase inhibitor Zanamivir.[2, 4, 6-11] However, both of these compounds are structurally complex requiring many-step syntheses to become amenable to attachment to polymeric chains in order to investigate the effect of multivalency.[2, 4] They are also difficult to modify selectively and thus not optimal for structure-activity relationship (SAR) studies. In the present work, we instead have employed simple organic molecules[12] with anti-influenza properties to investigate the SAR of multivalency. In particular,

we have assessed whether the aforementioned potential benefits of multivalency invariably translate into greater anti-influenza activity.

Materials and Methods

Materials

All small-molecule inhibitors except for **13** (Figure 1), poly-L-glutamate Na salt (50 -100 kDa), solvents, and reagents were purchased from Sigma-Aldrich Chemical Co. (St. Louis, MO) and used without further purification. Dialysis membranes (3,500 kDa molecular weight cutoff) were from Spectrum Labs (Rancho Dominguez, CA) and PD-10 desalting columns from GE Healthcare (Buckinghamshire, U.K.).

Syntheses

Synthesis of 6-(hydroxymethyl)naphthalene-1,4-dione (13) was carried out as described by Antonini et al.[13]

Synthesis of 2a, 2b, 5a, 5b, 8, 11, and 14: Conjugation was carried out via a Steglich esterification with minor deviations from a reported procedure.[14] Specifically, poly-L-glutamate Na salt was converted to poly(L-glutamic acid) by dissolution in double-distilled (dd) H_2O, lowering the pH to 1, and washing with 0.10 M HCl to remove free salts before an overnight lyophilization. Lyophilized poly(L-glutamic acid) (20 mg, 0.16 mmol) was dissolved in 0.80 mL of dry dimethylformamide (DMF), followed by the addition of *N,N'*-dicyclohexylcarbodiimide (DCC) (4.3 mg (0.021 mmol) in 0.30 mL of DMF for a ~10% derivatization), an anti-influenza agent (0.050 mmol in 0.20 mL of DMF), pyridine (10 μL, 0.12 mmol), and a catalytic quantity of 4-dimethylaminopyridine (DMAP) in 0.40 mL of DMF with vigorous stirring. The solution was

4

stirred overnight at room temperature. The polymer was then isolated by precipitation in chloroform, washed with fresh chloroform to remove the unreacted anti-influenza agent, converted to the Na salt, and dialyzed against ddH$_2$O in a 3,500-Da MW cutoff dialysis membrane for 24 hr to remove free salts and other impurities. TLC using a 3:1 (v/v) ethyl acetate:hexanes mixture confirmed purity and demonstrated the disappearance of the anti-influenza agent's spot. Percent conjugation of the anti-influenza agent was calculated by means of ^{1}H-NMR in D$_2$O using a Bruker 600 MHz instrument by comparing the ratio of the integration of a polymer peak with that of an anti-influenza agent's peak. In the case of a ~5% derivatization of the polymer with anti-influenza agent, 2.0 mg/0.010 mmol of DCC was added to the reaction mixture (**2b**, **5b**, and **11**).

^{1}H-NMR (D$_2$O) δ (600 MHz) — for **2a** and **2b**: 1.6-2.0 (2H polymer, d, CH$_2$), 2.1-2.5 (2H polymer, s, CH$_2$), 4.0-4.4 (1H polymer, s, CH), 6.8-8.0 (5H, aromatics); for **5a** and **5b**: 1.8-2.1 (2H polymer, d, CH$_2$), 2.1 (2H, m, cyclohexyl CH$_2$), 2.2-2.4 (2H polymer, s, CH$_2$), 2.6 (2H, m, cyclohexyl CH$_2$), 2.8 (2H, m, cyclohexyl CH$_2$), 4.2-4.4 (1H polymer, s, CH), 7.3-7.9 (3H, aromatics); for **8**: 1.6-2.0 (2H polymer, d, CH$_2$, 3H, s, CH$_3$), 2.1-2.5 (2H polymer, s, CH$_2$), 4.0-4.4 (1H polymer, s, CH), 7.5-8.0 (4H, aromatics); for **11**: 1.9-2.2 (2H polymer, d, CH$_2$), 2.3 (3H, s, CH$_3$), 2.4-2.5 (2H polymer, s, CH$_2$), 4.0-4.4 (1H polymer, s, CH), 6.9-8.2 (4H, aromatics); for **14**: 1.6-2.0 (2H polymer, d, CH$_2$), 2.0 (2H, s, CH$_2$), 2.0-2.3 (2H polymer, s, CH$_2$), 4.0-4.4 (1H polymer, s, CH), 6.7-8.0 (4H, aromatics).

Synthesis of 3, 6, 9, and 12: The conjugation of the anti-influenza agents to the polymer through a spacer arm was carried out via a Cu$^+$-catalyzed [3+2] azide-alkyne cycloaddition in three steps. First, poly-L-glutamate Na salt was derivatized with propargylamine as described by Ochs et al.[15] Next, anti-influenza agents were derivatized with a linker terminating with an azide

5

to be used in the subsequent cycloaddition. To this end, anti-influenza agent (0.30 mmol) was dissolved in 8 mL of dry dichloromethane, followed by the addition of azidopentanoic acid (50 µL, 0.40 mmol), *N,N′*-diisopropylcarbodiimide (DIC) (60 µL, 0.40 mmol), pyridine (50 µL, 0.60 mmol), and a catalytic quantity of DMAP. The reaction mixture was stirred overnight, concentrated by rotary evaporation, and purified by column chromatography (2:1 (v/v) hexanes:ethyl acetate) to generate such compounds as **15**. For the conjugation of anti-influenza agents to the polymer via cycloaddition, the alkyne-derivatized poly-L-glutamate Na salt (68 mg, 0.45 mmol) was dissolved in 1.5 mL of ddH$_2$O. The above-mentioned purified linker-derivatized anti-influenza agent (0.10 mmol) was dissolved in 1.5 mL of *tert*-butanol and added to the water/polymer mixture. A 1.0 M aqueous solution of Na ascorbate (75 µL) and a 0.10 M aqueous solution of CuSO$_4$ (50 µL) were then added; the reaction mixture was incubated overnight,[16] concentrated via rotary evaporation, dissolved in phosphate buffered saline (PBS), run on a PD-10 desalting column, and dialyzed as above to remove unreacted starting material and reagents. Polymer conjugates were analyzed as outlined above to quantify derivatization.

   ^{1}H-NMR (D$_2$O) δ (600 MHz) — for **3**: 1.5 (2H, m, CH$_2$), 1.7-2.1 (2H polymer, d, CH$_2$, 4H, m, CH$_2$), 2.1-2.5 (2H polymer, s, CH$_2$), 4.0-4.5 (1H polymer, s, CH, 4H, m, CH$_2$), 6.8-8.0 (6H, aromatics); for **6**: 1.7 (2H, m, CH$_2$), 1.8-2.1 (2H polymer, d, CH$_2$, 4H, m, CH$_2$), 2.1 (2H, m, cyclohexyl CH$_2$), 2.1-2.5 (2H polymer, s, CH$_2$), 2.6 (2H, m, cyclohexyl CH$_2$), 2.7 (2H, m, cyclohexyl CH$_2$), 4.2-4.5 (1H polymer, s, CH, 4H, m, CH$_2$), 7.2-8.0 (4H, aromatics); for **9**: 1.5 (2H, m, CH$_2$), 1.7-2.1 (2H polymer, d, CH$_2$, 4H, m, CH$_2$, 3H, s, CH$_3$), 2.1-2.5 (2H polymer, s, CH$_2$), 4.2-4.5 (1H polymer, s, CH, 4H, m, CH$_2$), 7.4-8.1 (4H, aromatics); for **12**: 1.6 (2H, m, CH$_2$), 1.7-2.1 (2H polymer, d, CH$_2$, 4H, m, CH$_2$, 3H, s, CH$_3$), 2.1-2.5 (2H polymer, s, CH$_2$), 4.2-4.5 (1H polymer, s, CH, 4H, m, CH$_2$), 6.5-8.0 (5H, aromatics).

Synthesis of 1-(5-((6-methyl-5,8-dioxo-5,8-dihydronaphthalen-1-yl)oxy)-5-oxopentyl)-1H-1,2,3-triazol-4-yl)methanaminium (16) was carried out similarly to the aforementioned cycloaddition. Briefly, 6-methyl-5,8-dioxo-5,8-dihydronaphthalen-1-yl 5-azidopentanoate (**15**) (33 mg, 0.10 mmol) was dissolved in 1.5 mL of *tert*-butanol. To that mixture, propargylamine (6.0 μL, 0.10 mmol) in 1.5 mL of ddH_2O was added, followed by the addition of a 1.0 M aqueous solution of Na ascorbate (75 μL) and a 0.10 M aqueous solution of $CuSO_4$ (50 μL). The reaction was stirred overnight, concentrated by rotary evaporation, and dissolved in ddH_2O. Following the addition of chloroform the aqueous fraction was recovered, dissolved in methanol, filtered, and concentrated for characterization by ^{1}H-NMR and for further use in biological assays.

^{1}H-NMR (MeOD) δ (400 MHz) for **16**: 1.6 (2H, m, CH_2), 2.0 (2H, m, CH_2, 3H, s, CH_3), 2.7 (2H, m, CH_2), 4.1 (2H, m, CH_2), 4.4 (2H, m, CH_2), 6.6 (1H, s, H3 aromatic), 7.3 (1H, d, H8 aromatic), 7.7 (1H, dd, H7 aromatic), 7.9 (1H, d, H6 aromatic), 8.1 (1H, s, NCHC).

Synthesis of 17 and 18: For **17**, poly-L-glutamate Na salt was activated with propargylamine as described above and then the remaining carboxylates were converted to their free acids by reducing the pH, followed by the removal of water by freeze-drying. The resultant compound (40 mg) was dissolved in 1.5 mL of DMF, then *N*-hydroxysuccinimide (NHS) (79 mg, 0.69 mmol) was added with stirring, and the temperature was reduced to 0 ºC, followed by an addition of DIC (108 μL, 0.69 mmol). The reaction mixture was stirred on ice for 30 min and at room temperature for 3 hr, after which time an excess of aqueous NH_4OH was added to displace the NHS-ester moieties resulting in a neutral poly-L-glutamine.[4, 17] Conjugation of **15** to the propargylamine-derivatized poly-L-glutamine was carried out via a cycloaddition as described above. For **18**, poly-L-glutamate Na salt was derivatized with propargylamine in the

same way as above, except that an excess of propargylamine (30 μL, 0.47 mmol) was added. For derivatization with inhibitor, the reaction was run as above, but only 0.1 mole-equivalents of **15** was used.

^{1}H-NMR (D$_2$O) δ (600 MHz) — for **17**: 1.6 (2H, m, CH$_2$), 1.8-2.2 (2H polymer, d, CH$_2$, 4H, m, CH$_2$, 3H, s, CH$_3$), 2.2-2.4 (2H polymer, s, CH$_2$), 4.2-4.5 (1H polymer, s, CH, 4H, m, CH$_2$), 6.4-8.0 (5H, aromatics); for **18**: 1.6 (2H, m, CH$_2$), 1.9-2.2 (2H polymer, d, CH$_2$, 4H, m, CH$_2$, 3H, s, CH$_3$), 2.2-2.5 (2H polymer, s, CH$_2$), 2.6 (1H, s, CH), 3.9 (2H, s, CH$_2$), 4.2-4.5 (1H polymer, s, CH, 4H, m, CH$_2$), 6.3-7.9 (5H, aromatics).

Cells, Viruses, and Antiviral Assays

Madin-Darby canine kidney (MDCK) cells were purchased from the American Type Culture Collection (ATCC) and maintained as described by Haldar et al.[2] The wild-type influenza A viruses Wuhan/359/95 (Wuhan) (H3N2) and turkey/MN/833/80 (turkey) (H4N2) were obtained from the U.S. Centers for Disease Control and Prevention (CDC), and the influenza A strain PR/8/34 (Puerto Rico) (H1N1) was purchased from Charles River Laboratories (North Franklin, CT). The viruses were stored at -80ºC and diluted in PBS prior to assays.

Plaque reduction assays with MDCK cells were conducted to determine the half-maximal inhibitory concentration (IC$_{50}$ value) for each compound tested using a literature methodology.[2, 4] For plaque reduction assays investigating the effect of inhibitor in the solid growth agar, equal concentrations of the inhibitor were used during pre-incubation, infection, and in the nutrient agar formulation.

Docking simulations

The hemagglutinin structures of the Puerto Rico and X-31 strains of influenza A virus were obtained from the Protein Data Bank (PDB: 1RU7 and 2HMG, respectively). The docking studies for the hemagglutinin proteins and compounds **10** and **16** were performed with AutoDock Vina[18] and AutoDock Tools interface. All rotatable bonds in the ligands were allowed to rotate freely using the default settings. The search area, selected based on the previous studies with influenza small-molecule hemagglutinin inhibitors,[12, 19] covered the majority of the grooves of the protein. The final results were selected based on the best binding modes.

Results and Discussion

Since the inherent structural complexities of Zanamivir and sialic acid do not allow for easy manipulations, for our SAR studies we chose to investigate whether there were simpler molecules also possessing anti-influenza activity. In the scholarly study by Bodian et al.,[12] expanded by others,[19] docking simulations were performed to discover small organic molecules that bind to the hemagglutinin protein on influenza A viral strain X31 (H3N2) and stabilize the protein in its native conformation. This stabilization was proposed to hinder the conformational changes necessary for cell-viral membrane fusion, which is an essential step in the influenza infection cycle.[12] Specifically, the binding site explored was a region approximately half-way between the most outer tip of the hemagglutinin protein and the viral membrane near the fusion peptide.[12] These docking studies resulted in a group of benzoquinones and hydroquinones as potential ligands to bind to hemagglutinin and to inhibit the aforementioned conformational change.[12]

9

One of the foregoing compounds, 5-hydroxynaphthalene-1,4-dione (**1**), was selected as a starting point for our studies. Using the plaque reduction assay method to test **1** for putative anti-influenza activity against the Wuhan strain of the influenza A virus, we indeed found it to be a moderate inhibitor with an IC_{50} value of 4.7 ± 1.5 µM (Table 1, 1st entry). While other unnatural anti-hemagglutinin inhibitors exist (figure 2),[20-25] all are structurally more complex than **1**. Therefore, we decided to continue our studies herein with compound **1**.

In light of the previous studies with polymer-attached Zanamivir and sialic acid,[2, 4, 6-11] we next tested whether covalent conjugation of multiple copies of **1** to a polymeric chain would increase anti-influenza potency. To this end, **1** was attached to the physiologically benign and biodegradable polymer poly-L-glutamate at a ~10% loading (*i.e.*, with approximately one tenth of all monomeric units being derivatized with the inhibitor). The resultant polymeric inhibitor **2a** exhibited an over 10-fold better IC_{50} value compared to its monomeric counterpart **1** (Table 1, 2nd entry), presumably due to the phenomenon of multivalency. Interestingly, lowering the degree of loading of the inhibitor on the polymer from 10% to 5% (to yield **2b**) failed to improve the antiviral potency (Table 1), suggesting that the polymer-conjugated ligand molecules do not interfere with each other's ability to inhibit the virus.

One can readily envisage how steric constraints imposed by the polymeric chain may hinder the ability of the inhibitor to bind to its viral receptor, thus masking the true power of multivalency. This hypothesis was verified by inserting a nine-atom spacer arm between the polymer and **1**, resulting in compound **3**. As seen in Table 1, this insertion indeed dramatically improved the IC_{50} value: 20-fold over **2a** and some 240-fold over **1**.

To examine the generality of these findings, several structural analogs of **1**, not previously identified as anti-influenza inhibitors,[12] were tested, along with their synthesized

poly-L-glutamate conjugates, against the Wuhan influenza strain. 5-Hydroxy-3,4-dihydronaphthalene-1(2H)-one (**4**) and 2-hydroxy-3-methylnaphthalene-1,4-dione (**7**) both were found to be inhibitors, albeit much weaker ones than **1**. Conjugating them to the polymer directly, *i.e.*, with no spacer arm (to produce **5a** or **5b** depending on the degree of loading and **8**, respectively) led to marked (7 and >3 fold, respectively) improvements in the antiviral potency (Table 1). Moreover, as seen in Table 1, when the nine-atom spacer arm was inserted to further distance the ligand from the polymeric chain (to form **6** and **9**, respectively), the inhibitory potency in both cases rose another several-fold to reach the overall improvement compared to those of the parents **4** and **7** of 38 fold and >140 fold, respectively.

The same general trend of a dramatically enhanced inhibitory potency upon attachment to the polymeric chain via the spacer arm was observed with yet another analog of **1** tested, namely 5-hydroxy-2-methyl-1,4-naphthalenedione (**10**). This compound, which differs from **1** only by a methyl substituent in the benzoquinone portion of the molecule, exhibited an IC_{50} value comparable to that of **1**; converting it to **12** produced a 52-fold jump in inhibitory activity (Table 1). Interestingly, however, in the case of **10** attached to the polymer with no spacer arm (**11**), no increase (and, in fact, a sizeable decline) in the potency was observed (Table 1), illustrating how subtle the SAR is.

The poly-L-glutamate conjugate of **13** (in the absence of a nine-atom linker), **14**, exhibited a greater than 30-fold improvement over its monomeric counterpart (Table 1) demonstrating that attachment through the 6C position in the naphthoquinone moiety does not have a deleterious effect on the inhibitor improvement; in fact, it generated the most potent non-linker conjugated inhibitor.

11

In addition to a striking improvement in the inhibitory potency of the ligands upon conjugating them to poly-L-glutamate via the long spacer arm, their toxicity also diminished. In particular, both for **2a**, **2b**, and **3** *vs*. **1** and for **11** and **12** *vs*. **10** the cellular toxicity was at least an order of magnitude lower. For example, when compound **1** was used in the infection phase of the plaque reduction assay, cells that were incubated with the concentrations of inhibitor greater than, or equal to, 30 μM displayed obvious fatal demise. In contrast, cells incubated with even greater than 300 μM concentrations of polymer-attached inhibitors **2a**, **2b**, and **3** were healthy and seemingly unaffected by the presence of inhibitor. Presumably, sequestering the toxic small molecules (50% cell cytotoxicity concentration, CC_{50}, of ~30 μM for **1**[12]) to the polymer prevents them from traversing the cellular membrane and exerting deleterious effects within the cell.

To determine to what extent the foregoing findings apply to other influenza A viruses, we selected two additional strains, namely the avian turkey and the human Puerto Rico ones. Both strains have different serotypes of the hemagglutinin and neuraminidase proteins compared to Wuhan's, leading to subtle differences in the amino acid makeup and structure of these proteins.[26] Using the plaque reduction assay, we tested the monomeric inhibitors **1**, **7**, **10**, and **13**, as well as those attached to poly-L-glutamate either via the nine-atom spacer arm (compounds **3**, **6**, and **12**) or directly (**14**). As in the case of the Wuhan strain, **1**, **10**, and **13** were substantial inhibitors of the viruses, whereas **7** was not (Table 2), suggesting similarities in the receptors' binding sites of all three strains. And yet, in stark contrast to the observations made with the Wuhan strain (Table 1), conjugation to the polymeric chains even via a long spacer arm not only failed to result in a significant improvement of the anti-influenza potency but, in the case of **1** and **10**, actually made it markedly worse, i.e., increased the IC_{50} values (Table 2). For **14**,

conjugation of the inhibitor to the polymer though the C6 position in the naphthoquinone also caused a substantial deterioration in potency for both turkey and Puerto Rico strains suggesting that the site of the linker's attachment is not entirely responsible for the reduction in inhibition.

We hypothesized that perhaps the addition of the linker group itself imposed new steric hindrances for binding of the inhibitor to the receptor sites on the turkey and Puerto Rico, but not the Wuhan, strains of the virus. This would inevitably lead to a diminished ability of the inhibitor to bind to its receptor when subsequently attached to poly-L-glutamate. To test this hypothesis, we focused on the compound **10** group of inhibitors and synthesized compound **16** containing the same chemical structure as the inhibitor plus the spacer arm portion of **12** but in the absence of polymer. As seen in Table 3, **16** indeed exhibited a drastically poorer anti-influenza inhibition against all three viruses compared to the parent compound **10**.

Thus the deteriorated inhibition potency upon attachment of the nine-atom spacer arm indeed may account for at least some of the inferior inhibition observed for compounds **3**, **9**, and **12** compared to their monomeric precursors **1**, **7**, and **10**, respectively, against the turkey and Puerto Rico strains. However, in order for **12** to exhibit the multivalency benefits over **16** of greater than 100 fold (as it did with Wuhan strain, Table 3), the IC_{50} value of **16** would have to be at least 10^4 μM for the Puerto Rico and turkey strains. The results of the plaque reduction assay suggest that this is not the case though: a reduction in plaque numbers for both of these strains upon incubation with 90 μM **16** indicated that the IC_{50} was close to 100 μM (data not shown). The exact IC_{50} for **16** was not measurable however, due to cytotoxicity of the compound.

Next we investigated the role of the polymer's charge in antiviral activity. To this end, two new polymer conjugates with compound **10** attached via the nine-atom spacer arm (**17** and

13

18) were prepared and tested against the Wuhan and turkey strains. Compound **17**, containing a neutral poly-L-glutamine backbone, showed modest improvements for the turkey strain over its negatively charged analog **12** but failed to exhibit a great enhancement over the monomer **10** (Table 4). Conversely, for the Wuhan strain, **17** demonstrated an almost 50-fold improvement over the monomer, similar to that afforded by compound **12** (Table 4). Likewise, compound **18** (containing a partly negatively charged backbone) displayed no great enhancement for the turkey strain while exhibiting an almost 40-fold improvement over **10** for the Wuhan strain. These results indicate that the charge on the polymeric chain cannot account for the striking differences observed between the turkey and Wuhan strains for monomeric *vs.* polymer-attached inhibitors.

To determine whether the difference in improvements for polymer-attached conjugates over monomeric inhibitors between the Wuhan and turkey strains was an artifact of our biological assay, i.e., whether the inhibitor was brought into contact with the virus at the inappropriate time during infection, we performed an additional plaque assay with **10** and **12** present not only during the pre-incubation and binding (as is conventionally done) but also with the inhibitor in the agar overlay. This modality of the plaque reduction assay exposes cells and viruses to the inhibitor for the entirety of the first and subsequent infection phases leaving the inhibitor available for all steps in the viral cycle and not just for binding or endocytosis. In this experimental mode, the inhibitory effect of **10** and **12** for the Wuhan strain changed only modestly: IC_{50}'s of 2.4 ± 0.39 µM and 0.061 ± 0.045 µM, respectively, for incubation of inhibitor in the agar overlay *vs.* 5.7 ± 1.7 µM and 0.11 ± 0.070 µM for our conventional experiment. For the turkey strain, the inhibition by the monomer (**10**) improved more (IC_{50} of 17 ± 1.0 µM when not included in the agar and 2.9 ± 0.49 µM when included in the agar) but the polymer-attached inhibitor's (**12**'s) IC_{50} exceeded 5 µM; these observations confirm that the lack

14

of improvement for polymer-attached inhibitors against the turkey strain was <u>not</u> an artifact of our biological assay.

We then hypothesized that the preferred binding sites of the monomeric *vs.* the polymer-attached inhibitors might be distinct between the strains, thus being responsible for their vastly different inhibitory properties. To explore this possibility, we ran *in silico* docking experiments to determine the preferred binding sites for the monomeric inhibitor **10** and the linker-attached inhibitor **16** for the Puerto Rico strain and a Wuhan surrogate strain, X-31 (both H3N2). Note that the X-31 strain has a 87% sequence identity for the HA1 strand of the hemagglutinin molecule compared to the Wuhan strain (the HA2 Wuhan sequence is unavailable)[27, 28] (for comparison, the Puerto Rico's HA1 strand has just a 33% sequence identity[29]). As seen in Figure 4A, for the X-31 strain both inhibitors bind in the same region of the hemagglutinin protein; this region coincides with the crystallographically determined binding site for *tert*-butyl hydroquinone (another fusion inhibitor described by Bodian et al.[12, 19]). In stark contrast, for the Puerto Rico strain, inhibitors **10** and **16** bind in vastly distinct locations on the hemagglutinin protein, with as much as 40 Å separating them (Fig. 4B). Note that **10** binds to a similar location on the Puerto Rico strain's hemagglutinin as both **10** and **16** in the X-31's protein; however, **16** on the Puerto Rico strain's hemagglutinin binds in a region that is closer to the viral envelope, thereby possibly hindering accessibility for the polymer-attached inhibitor.

One has to wonder why there are benefits of multivalency for all the compounds tested attached via a long spacer arm to a poly-L-glutamate for one strain of influenza, but not for the other two (Tables 1 and 2). It is unlikely that the observed differences in inhibition among viral strains are due to dissimilar spacing of hemagglutinin molecules along the viral surface among different strains. There ~400 hemagglutinin molecules on a given viral particle of roughly the

same size regardless of the influenza virus strain. Since the mechanism of viral particle formation is the same for different strains, the spacing among hemagglutinin molecules on average should be similar as well.[26] The binding of the first polymer-attached inhibitor molecule to hemagglutinin is also unlikely to prevent binding of all the others. Although the binding of the first inhibitor molecule indeed might make it sterically impossible for a second, nearby counterpart to bind to hemagglutinin, that cannot be the case for more distant polymer-attached inhibitor molecules. Since our (~10%-derivatized) polymeric chain contains some 50 randomly distributed inhibitor molecules, most of them should be sufficiently remote from the first one bound to interact with another hemagglutinin molecule.

The three influenza strains undoubtedly have some differences in the binding site for these inhibitors;[26] in the case of the turkey and Puerto Rico strains, these differences might interplay with the polymer and/or linker deleteriously to weaken the binding of the conjugated inhibitor to the virus. Additionally, the topology of the viral surface might introduce accessibility problems for the inhibitors once they are attached to the bulky, hydrated polymeric chain. In previous studies of the effect of multivalency on anti-influenza inhibitors, the receptor of the multivalent ligand was proximal to the solvent-exposed outer edge of the surface protein.[2, 4, 6-11] Although the exact location of binding of **1** and its analogs to hemagglutinins in the strains studied herein is unknown, our docking studies (Fig. 4) predict that for **10** and **16** the site is located approximately half-way down the protein for the X-31 strain and close to the viral envelope for the linker-attached inhibitor (**16**) on the Puerto Rico strain.[12] Perhaps while a small molecule readily accesses regions down the stock of the protein, conjugation to a bulky polymeric chain hampers the access below the dense canopy of proteins on the viral surface.

16

The concept of multivalency stipulates that several simultaneous interactions of ligands and receptors should result in a stronger, multipoint inhibitor-virus binding and hence give rise to more potent inhibitors (Figure 5).[6] Our results herein suggest, however, that this is indeed the case only if attaching an inhibitor to a polymeric chain does not impose negative spatial constraints not outweighed by the inherent benefits of multivalency. Since it is unknown in advance whether this will be the case, our data illustrate that the superiority of multivalent inhibitors of a virus compared to their monovalent predecessors cannot be automatically assumed.

Acknowledgements

References

1. Grahm-Rowe D. 2011. Racing against the flu. Nature 480:S2-S3.

2. Haldar J, Alverez de Cienfuegos L, Tumpey TM, Gubareva LV, Chen J, Klibanov AM. 2010. Bifunctional polymeric inhibitors of human influenza A viruses. Pharm Res 27:259-263.

3. Palmer R. 2011. Lines of defense. Nature 480:S9-S10.

4. Weight A, Haldar J, Alverez de Cienfuegos L, Gubareva LV, Tumpey TM, Chen J, Klibanov AM. 2011. Attaching Zanamivir to a polymer markedly enhances its activity against drug-resistant strains of influenza. J Pharm Sci 100:831-835.

5. Gubareva LV. 2004. Molecular mechanism of influenza virus resistance to neuraminidase inhibitors. Virus Res 103:199-203.

6. Mammen M, Choi SK, Whitesides GM. 1998. Polyvalent interactions in biological systems: implications for use of multivalent ligands and inhibitors. Angew Chem Int Ed 37:2754-2794.

7. Mammen M, Dahmann G, Whitesides GM. 1995. Effective inhibitors of hemagglutination by influenza virus synthesized from polymers having active ester groups. Insight into mechanism of inhibition. J Med Chem 38:4179-4190.

8. Choi SK, Mammen M, Whitesides GM. 1997. Generation and *in situ* evaluation of libraries of poly(acrylic acid) presenting sialosides as side chains as polyvalent inhibitors of influenza-mediated hemagglutination. J Am Chem Soc 119:4103-4111.

9. Sigal G, Mammen M, Dahmann G, Whitesides GM. 1996. Polyacrylamides bearing pendant α-sialoside groups strongly inhibit agglutination of erythrocytes by influenza virus: the strong inhibition reflects enhanced binding through cooperative polyvalent interactions. J Am Chem Soc 118:3789-3800.

10. Masuda T, Yoshida S, Arai M, Kaneko S, Yamashita M, Honda T. 2003. Synthesis and anti-influenza evaluation of polyvalent sialidase inhibitors bearing 4-guanidino-Neu5Ac2en derivatives. Chem Pharm Bull 51:1386-1398.

11. Carlescu I, Scutaru D, Popa M, Uglea CV. 2009. Synthetic sialic-acid-containing polyvalent antiviral inhibitors. Med Chem Res 18:477-494.

12. Bodian DL, Yamasaki RB, Buswell RL, Stearns JF, White JM, Kuntz ID. 1993. Inhibition of the fusion-inducing conformational change of influenza hemagglutinin by benzoquinones and hydroquinones. Biochemistry 32:2967-2978.

13. Antonini I, Lin TS, Cosby LA, Dai YR, Sartorelli AC. 1982. 2- and 6-methyl-1,4-naphthoquinone derivatives as potential bioreductive alkylating agents. J Med Chem 25:730-735.

14. Li C, Yu DF, Newman RA, Cabral F, Stephens LC, Hunter N, Milas L, Wallace S. 1998. Complete regression of well-established tumors using a novel water-soluble poly(L-glutamic acid) paclitaxel conjugate. Cancer Res 3:2404-2409.

15. Ochs C, Such G, Stadler B, Caruso F. 2008. Low-fouling, biofunctionalized and biodegradable click capsules. Biomacromolecules 9:3389–3396.

16. Jia Z, Zhu Q. 2010. 'Click' assembly of selective inhibitors for MAO-A. Bioorg Med Chem Lett 20:6222-6225.

17. Song Y, Goel A, Basrur V, Roberts P, Mikovits J, Inman J, Turpin J, Rice W, Appella E. 2002. Synthesis and biological properties of amino amide ligand-based pyridinoalkanoyl thioesters as anti-HIV agents. Bioorg Med Chem 10:1263-1273.

18. Trott O, Olson AJ. 2010. AutoDock Vina: improving the speed and accuracy of docking with a new scoring function, efficient optimization and multithreading. J Comp Chem 31:455-461.

19. Russel R, Kerry P, Stevens D, Steinhauer D, Martin S, Gamblin S, Skehel J. 2008. Structure of influenza hemagglutinin in complex with an inhibitor of membrane fusion. Proc Natl Acad Sci USA 105:17736-17741.

20. Guo CT, Sun XL, Kaine O, Shortridge KF, Suzuki T, Miyamoto D, Hidari KI, Wong CH, Suzuki Y. 2002. An *O*-glycoside of sialic acid derivative that inhibits both hemagglutinin and sialidase activities of influenza viruses. Glycobiol 12:183-190.

21. Vanderlinden E, Goktas F, Cesur Z, Froeyen M, Reed M, Russell C, Cesur N, Maesens L. 2010. Novel inhibitors of influenza virus fusion: structure-activity relationship and interaction with the viral hemagglutinin. J Virol 84:4277-4288.

22. Luo G, Colonno R, Krystal M. 1996. Characterization of a hemagglutinin-specific inhibitor of influenza A virus. Virol 226:66-76.

23. Tang G, Qiu Z, Lin X, Li W, Zhu L, Li S, Li H, Wang L, Chen L, Wu J, Yang W. 2010. Discovery of novel 1-phenyl-cycloalkane carbamides as potent and selective influenza fusion inhibitors. Bioorg Med Chem Lett 20:3507-3510.

24. Staschke KA, Hatch SD, Tang JC, Hornback WJ, Munroe JE, Colacino JM, Museing MA. 1998. Inhibition of influenza virus hemagglutinin-mediated membrane fusion by a compound related to podocarpic acid. Virol 248:264-274.

25. Plotch SJ, O'Hara B, Morin J, Palant O, LaRocqur J, Bloom JD, Lang SA, DiGrandi MJ, Bradley M, Nilakantan R, Gluzman Y. 1999. Inhibition of influenza A virus replication by compounds interfering with the fusogenic function of the viral hemagglutinin. J Virol 73:140-151.

26. Knipe DM, Howley PM. 2007. Fields' Virology. In Lamb RA, Krug, RM, editors. *Orthomyoxoviridae*: The Viruses and Their Replication, 5th ed., Philadelphia: Wolters Kluwer Health/Lippincott Williams & Wilkins. Pp. 1492-1496.

27. Russell CA, Jones TC, Barr IG, Cox NJ, Garten RJ, Gregory V, Gust I.D, Hampson AW, Hay AJ, Hurt AC, de Jong JC, Kelso A, Klimov AI, Kageyama T, Komadina N , Lapedes AS, Lin YP, Mosterin A, Obuchi M, Odagiri T, Osterhaus AD, Rimmelzwaan GF, Shaw MW, Skepner E, Stohr K, Tashiro M, Fouchier RA, Smith DJ. 2008. The global circulation of seasonal influenza A (H3N2) viruses. Science 320:340-346.

28. Ward CW, Dopheide TA. 1981. Amino acid sequence and oligosaccharide distribution of the haemagglutinin from an early Hong Kong influenza virus variant A/Aichi/2/68 (X-31). Biochem J 193:953-962.

29. Winter G, Fields S, Brownlee GG. 1981. Nucleotide sequence of the haemagglutinin gene of a human influenza virus H1 subtype. Nature 292:72-75.

<u>Figure Legends</u>

Figure 1. Chemical structures of (A) 5-hydroxynaphthalene-1,4-dione (**1**) and its analogs **4**, **7**, **10**, and **13** used in this study; (B) modified **10** with an azide-terminated spacer arm (**15**) for use in conjugating to propargylamine-derivatized poly-L-glutamate and **10** derivatized with a spacer arm (**16**) for investigation of the dependence of IC_{50} on the presence of the spacer arm by itself with no polymer.

Figure 2. Chemical structures of anti-hemagglutinin agents previously described in the literature: (A) Neu5Ac3αF-DSPE;[20] (B) *N*-(2,8-dimethyl-3-oxo-1-thia-4-azaspiro[4.5]decan-4-yl)-6-methylimidazo[2,1-b]thiazole-5-carboxamide;[21] (C) 4-amino-5-chloro-2-hydroxy-*N*-((2S,6R,9aR)-6-methyloctahydro-1H-quinolizin-2-yl)benzamide;[22] (D) *N*-(3-cyanophenyl)-*N*-methyl-2-phenylcyclohexanecarboxamide;[23] (E) methyl-*O*-methyl-7-ketopodocarpate;[24] (F) 3-fluoro-*N*-(2-(piperidin-1-yl)ethyl)-5-(trifluoromethyl)benzamide [25]. It is worth noting that **1** is a more potent anti-influenza inhibitor than compound F (IC_{50} of 315 μM),[25] on par with compounds A, B, and C

21

(IC$_{50}$'s of 5.6, 3-23, and 3-8 μM, respectively),[20-22] and less potent than compounds D and E (IC$_{50}$'s of 98 and 31 nM, respectively).[23,24]

Figure 3. Chemical structures of anti-influenza inhibitors attached to poly-L-glutamate (A) with no spacer arm; (B) via a nine-atom spacer arm intended to reduce the putative steric hindrances imposed by the polymeric chains; (C) with the polymeric backbone of varying degrees of electrostatic charge.

Figure 4. The docking results for inhibitors **10** and **16** (both black) on the hemagglutinin protein (grey) of the X-31 strain (a surrogate used to represent the Wuhan strain) (A, left panel) and of the Puerto Rico strain (B, right panel) of influenza A virus. As seen in A, the binding sites on the protein for the two inhibitors overlap in the former case. In contrast, the distance between the binding sites for the two inhibitors in B is some 40 Å indicating that the molecules bind to the protein in vastly distinct locations. The images, generated in Pymol, depict only **10** and **16** docked on one hemagglutinin monomer for each viral strain.

Figure 5. A cartoon depicting a multivalent *vs.* a monovalent interaction of an inhibitor with the virus. The top panel (A) depicts a polymer-attached inhibitor (polymer is black line, inhibitors are open circles) interacting with a viral envelope containing the receptors of the inhibitor (grey part-circle is the viral envelope, white open half-circles are receptors, dotted lines indicate a binding interaction). Attaching multiple copies of the inhibitor to a polymeric chain can result in a multivalent and hence much stronger interaction with the viral receptors. The bottom panel (B) depicts a monovalent interaction of parent inhibitor molecules with a viral receptor. In this case, the individual inhibitor molecules act independently of each other in binding to their receptors and hence do not benefit from entropically enhanced binding (i.e., from multivalency).

Table 1. IC$_{50}$ values for both small molecules and their polymer-attached derivatives against the Wuhan strain of influenza A virus.

Inhibitor	IC$_{50}$ (μM)[a]
1	4.7 ± 1.5
2a	0.40 ± 0.20
2b	0.87 ± 0.14
3	0.020 ± 0.006
4	95 ± 22
5a	13 ± 7.2
5b	13 ± 2.7
6	2.5 ± 1.6
7	>100
8	33 ± 7.0
9	0.72 ± 0.21
10	5.7 ± 1.7
11	18 ± 10
12	0.11 ± 0.070
13	5.7 ± 0.70
14	0.18 ± 0.010

[a] The plaque reduction assay experiments were run at least in triplicate; the calculated mean and standard deviation values are presented in the table. The IC$_{50}$ values are expressed based on the concentration of the small-molecule inhibitor. The IC$_{50}$ value of bare poly-L-glutamate was found to exceed 1 mM and thus should not appreciably contribute to the extent of inhibition.

Table 2. IC$_{50}$ values for both small molecules and their polymer-attached derivatives against the Puerto Rico and turkey strains of influenza A virus.

Inhibitor	IC$_{50}$ (μM)^a	
	Puerto Rico	turkey
1	13 ± 1.6	4.7 ± 1.6
3	140 ± 45	84 ± 23
7	>100	>100
9	99 ± 16	100 ± 5
10	14 ± 1.6	17 ± 1
12	150 ± 10	53 ± 20
13	14 ± 1.0	5.3 ± 2.3
14^b	120 ± 19	>298

^{a} The plaque reduction assay experiments were run at least in triplicate; the calculated mean and standard deviation values are presented in the table. The IC$_{50}$ values are expressed based on the concentration of the small-molecule inhibitor. The IC$_{50}$ values for compounds **4** and **6** exceeded 170 μM for both viral strains. Thus they were not included in this table because no definitive conclusions concerning the effect of attachment to the polymer can be made. ^{b} All polymer conjugates characterized in this table contain the nine-atom spacer arm, except for **14** which comprises **13** conjugated directly to poly-L-glutamate.

<u>Table 3.</u> IC$_{50}$ values for compounds 10, 12 and 16 against three influenza A virus strains

Inhibitor	IC$_{50}$ (μM)^a		
	Wuhan	Puerto Rico	turkey
10	5.7 ± 1.7	14 ± 1.6	17 ± 1
12	0.11 ± 0.070	150 ± 10	53 ± 20
16	45 ± 8	$>100^b$	$>100^b$

^{a} The plaque reduction assay experiments were run at least in triplicate; the calculated mean and standard deviation values are presented in the table. The IC$_{50}$ values are expressed based on the concentration of the small-molecule inhibitor. ^{b} Although the IC$_{50}$ values for the turkey and Puerto Rico strains could not be conclusively determined because the 50% cell cytotoxicity concentration (CC$_{50}$) for **16** only slightly exceeded 100 μM, there was a visible reduction in plaques upon incubation with 90 μM of **16**.

Table 4. Comparison of IC$_{50}$ values for inhibitors conjugated to polymers of varying degrees of backbone charge against the Wuhan and turkey strains of influenza A virus.

Inhibitor	IC$_{50}$ (μM)^a	
	Wuhan	turkey
12	0.11 ± 0.070	53 ± 20
17	0.12 ± 0.061	7.4 ± 3.9
18	0.15 ± 0.035	35 ± 9.0

^{a} The plaque reduction assay experiments were run at least in triplicate; the calculated mean and standard deviation values are presented in the table. The IC$_{50}$ values are expressed based on the concentration of the small-molecule inhibitor.
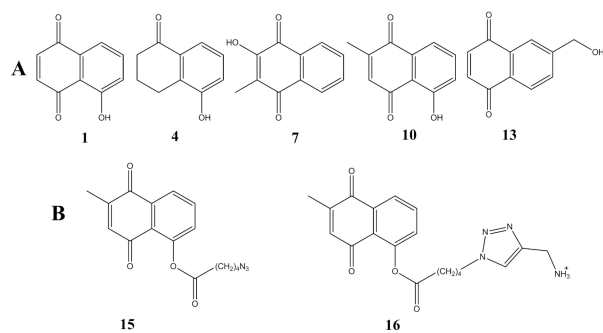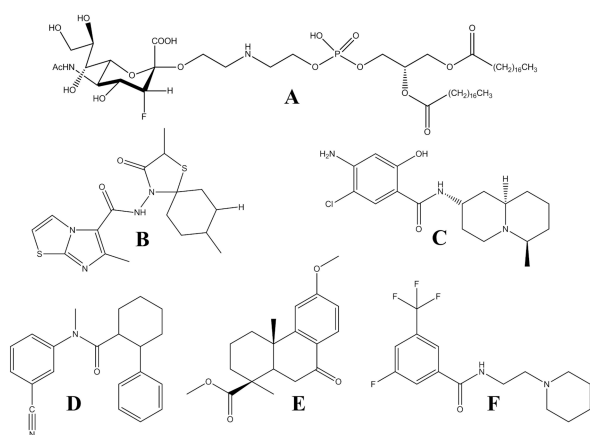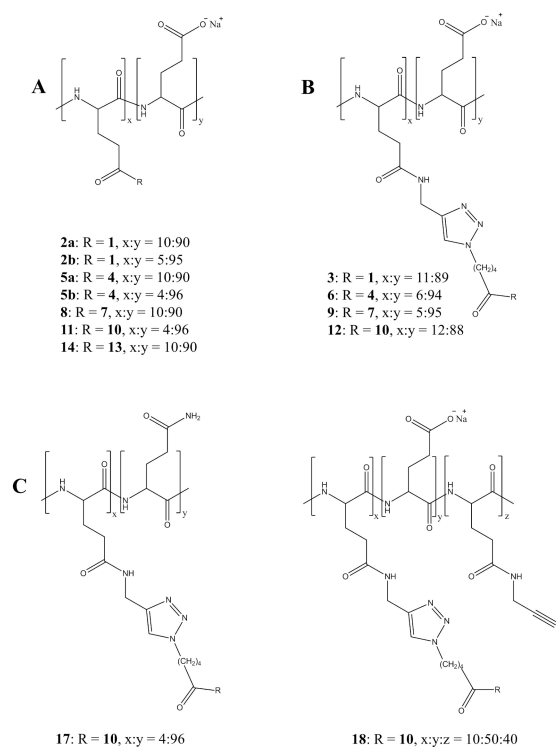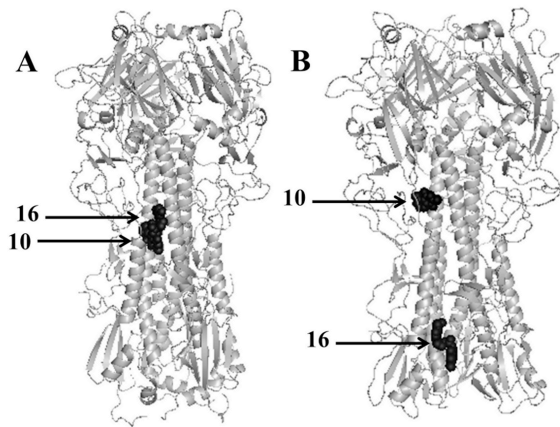
Figure 1

Figure 2

Figure 3

2a: R = **1**, x:y = 10:90
2b: R = **1**, x:y = 5:95
5a: R = **4**, x:y = 10:90
5b: R = **4**, x:y = 4:96
8: R = **7**, x:y = 10:90
11: R = **10**, x:y = 4:96
14: R = **13**, x:y = 10:90

3: R = **1**, x:y = 11:89
6: R = **4**, x:y = 6:94
9: R = **7**, x:y = 5:95
12: R = **10**, x:y = 12:88

17: R = **10**, x:y = 4:96

18: R = **10**, x:y:z = 10:50:40

27

Figure 4

Figure 5